CODEN [USA]: IAJPBB ISSN: 2349-7750

INDO AMERICAN JOURNAL OF
PHARMACEUTICAL SCIENCES

SJIF Impact Factor: 7.187

https://zenodo.org/records/10854649

https://www.iajps.com/volumes/volume11-march-2024/06-issue-03-march-24/

Available online at: http://www.iajps.com *Review Article*

# "NANO-QSAR MODELING FOR PREDICTING THE TOXICITY OF METAL-BASED METAL OXIDE NANOPARTICALS: AN IN-DEPTHEXPLORATION"

**[1]D.Pravallika, [2]Dr.J.Gopala Krishna**

[1]Student of Dr.K.V.subbareddy Institute of Pharmacy

[2]M.S Pharm,Ph.D., Associate Professor, Department of Pharmaceutical Chemistry
Dr.K.V.Subbareddy Institute of Pharmacy

**Abstract:**

*A variety number of nanoparticles will increase rapidly in coming years and there is a need for new methods to test the toxicity of the materials. Now a days experimental evaluation of the safety of chemicals is expensive and time consuming. Computational nano QSAR modelshave been found to be efficient alternatives for predicting the toxicity of metal oxide nano particles.*

*The present study proposes a computational QSAR models for predicting the toxicity of MEONPs. Two types of mechanisms are collectively applied in a nano QSAR model,which provides control over the toxicity of metal oxide nanoparticles. The two parameters, enthalpy of formation of gaseous cation (ΔHme+) and polarization force(Z/r) were elucidated to make a significant contribution for the toxic effect of the metal oxide nanoparticles.*

**Corresponding author:**

**Dr.J.Gopala Krishna,**

*M.S.Pharm,Ph.D,*

*Associate Professor, Department of Pharmaceutical Chemistry,*

*Dr.K.V.Subbareddy Institute Of Pharmacy,*

QR CODE

*Please cite this article in press J.Gopala Krishna et al.,* **Nano-QSAR Modeling For Predicting The Toxicity Of Metal-Based Metal Oxide Nanoparticles: An In-DepthExploration,**, *Indo Am. J. P. Sci, 2024; 11 (03).*

## INTRODUCTION:

Metal-based and metal oxide nanoparticles have become integral components in an array of consumer products and industrial applications. Their unique physicochemical properties offer numerous advantages, yet the assessment of their potential toxicity is a critical consideration in their safe utilization [1]. These nanoparticles, particularly metal oxide nanoparticles, hold a substantial share in various sectors, encompassing information technology, healthcare, transportation, and construction, constituting approximately 80% of the market volume. Metaloxide nano particles have wide range of technological applications like gas sensors, photovoltaics, adsorbents, catalysis and fuel cells due to their unique superparamagnetic, piezoelectric, optical, etc. properties [2]

However, understanding the toxicity mechanisms of these nanoparticles is a complex endeavour. Factors such as nanoparticle size, shape, crystal structure, and dosage all play intricate roles in their potential harm [3]. Notably, certain nanoscale metal oxide nanoparticles, including Cuo and Zno exhibit a heightened degree of toxicity when compared to carbon nanoparticles and multi-walled carbon nanotubes. Inflammatory responses, among other factors, are critical drivers of these toxic effects, influencing both organism-level and cellular- level responses. [4]

In light of these complexities, the development of nano-QSAR (Quantitative Structure-Activity Relationship) models has emerged as a valuable tool for predicting and understanding the toxicity of metal-based and metal oxide nanoparticles. [5].The first Nano-QSAR model designed to predict the cytotoxicity of metal oxide nanoparticles was introduced by Puzyn et al[6].

Nano-QSAR entails a statistical approach that seeks to establish quantitative relationships between independent variables, which encompass the physicochemical properties of these nanoparticles, and dependent variables, signifying their toxic effects.[7] Over the past decade, substantial progress has been made in modeling various nanoparticle properties, employing QSAR methodologies.[8] The term "nano-QSAR" specifically denotes the pursuit of quantitative connections between nanoparticle features and their effects on specific target activities.[9] Multiple nano-QSAR models, concentrating on both metallic and metal oxide nanoparticles, have been developed to predict their toxicity.[10]

This comprehensive article provides an extensive exploration of the applications and significance of nano-QSAR modeling in comprehensively assessing, predicting, and understanding the toxicity of metal-based and metal oxide nanoparticles, ultimately contributing to the responsible and informed use of these nanomaterials across various industries. [11]
Relying on the type of experimental data, QSAR can predict the physical and chemical properties and toxic influences of new compounds. Formerly, nano-QSAR has been developed to predict solubility, partition coefficient and young's modulus. But now we can apply nano- QSAR to predict toxicity of nanoparticles. [12]

| Metal oxide | Descriptor $\Delta H_{Me+}$(kcal$mol^{-1}$) | Leverage value, h | Observed log 1/EC50($mol^{-1}$) | Predicted log 1/EC50($mol^{-}$) | Residuals | set |
|---|---|---|---|---|---|---|
| Zno | 662.44 | 0.33 | 3..45 | 3.30 | 0.15 | T |
| Cuo | 706.25 | 0.29 | 3.20 | 3.24 | -0.04 | T |
| V2O3 | 1097.73 | 0.11 | 3.14 | 2.74 | 0.40 | V1 |
| Y2O3 | 837.15 | 0.21 | 2.87 | 3.08 | -0.21 | T |
| Bi2O3 | 1137.40 | 0.10 | 2.82 | 2.69 | 0.13 | T |
| In2O3 | 1271.13 | 0.10 | 2.81 | 2..52 | 0.29 | T |
| Sb2O3 | 1233.06 | 0.10 | 2..64 | 2.57 | 0.07 | V1 |
| Al2O3 | 1187.83 | 0.10 | 2.49 | 2.63 | -0.14 | T |
| Fe2O3 | 1408.29 | 0.13 | 2.29 | 2.35 | 0.06 | T |
| SiO2 | 1686.38 | 0.26 | 2.20 | 1.99 | 0.21 | T |
| ZrO2 | 1357.66 | 0.11 | 2.15 | 2.41 | 0.26 | V1 |
| SnO2 | 1717.32 | 0.28 | 2.01 | 1.95 | 0.06 | T |
| TiO2 | 1575.73 | 0.19 | 1.74 | 2.13 | -0.39 | T |
| CoO | 601.80 | 0.38 | 3.51 | 3.38 | 0.13 | $V^2$ |
| NiO | 596.70 | 0.39 | 3.45 | 3.38 | -0.07 | $V^2$ |

Table1: structure and toxicity data

The Nano QSAR were developed using descriptors, which were calculated by combining the molecular descriptors of the components of the mixture in a component-based approach. [13]

Based on the toxicity data and structural descriptors, we can write a simple and significant Nano-QSAR equation, using only one descriptor to predict the concentration of a compound.
[14]

$$\log(1/EC_{50}) = 2.59 - 0.50 \cdot \Delta H_{Me+}$$

Where $\Delta H_{Me+}$ enthalpy of formation of a gaseous cation having the same oxidation state asthat in the metal oxide structure

$$Me(s) \rightarrow Me^{n+}(g) + n \cdot e \; \Delta H_{Me+}$$

The table represents experimental and predicted data related to the toxicity of the studied nanomaterials in terms of EC50.The predicted EC50 values were calculated a single descriptor,Δ H Me+. The nanomaterials are denoted by T, and validation sets by V1 and V2. The leveragevalue h indicates deviations of the structure of the compound from those used for the QSAR development. The data given in the below table indicates that Zn O, Cu O, Nio and CoO nanoparticles exhibit the highest toxicity with TiO2 nanoparticles being the least toxic. [6]

**Biological data and nanoscale structural properties:**
Data on the toxic potencies of Metal oxide nanoparticles were obtained from the literature and laboratory experiments that were expressed in terms of the negative logarithm of EC50 (mol/L) [6,8]. Twenty-six physicochemical properties of metal oxide nanoparticles were calculated, which contained physicochemical, scale, and thermodynamic properties of both nanoparticles and metal ions. Calculations were made at the semi-empirical theoretical level using PM6 methods. [6]

The descriptors could reliably reflect various properties of metal oxide nanoparticles, which included enthalpy of formation of a gaseous cation, energy difference and standard heat of formation. [6]

Twenty-three properties of metal ions released from the MeOxNPs included:

softness index (σp), ionic charge (Z), softness index per ion charge (σp/Z) atomic number (AN), difference in ionization potentials between the O(N +1) state and ON state (IP) of the ion (ΔIP), and atomic ionization potential (AN/ΔIP) ,electro negativity (Xm), Pauling ionic radius(r), and covalent index (X $^{2}$r); electrochemical potential (ΔE ); first hydrolysis constants, relative softness(Z/rx) where x represents electro negativity values, atomic radius (AR), atomic weight (AW), and electron density (AR/AW) ; polarization force parameters (Z/r, $Z/r^2$and $Z^2/r$), and similar polarization force parameters (Z/AR and $Z/AR^2$) .[15]

The above descriptors are size-independent, which seems to be in conflict with the widely accepted notion that the size of MeONPs is decisive for their toxicity.[6]

The variation of property with the increasing size of the nanomaterials does not occur until it reaches the saturation point. Therefore, we assumed that the clusters must be of the same size and bigger than 5nm for all the studied oxides.

**Methods:**

**Empirical toxicity testing**:
Empirical methods are much faster than quantum-mechanical ab initio methods allow calculations of larger systems to be carried out, but their accuracy is often disputed.

From a quantum-mechanical point of view, calculations for nanoparticles with a size of 15–90nm were not feasible (the systems are too large), so it was necessary to maximally simplify thestructural models used to calculate the descriptors. We calculated the descriptors using smaller metal oxide fragments (clusters) of the same size for all nanoparticles and one descriptor, based on the characteristics of the considered metal atoms. [16]

The two types of the nanoparticles that were tested empirically, Mn2O3 (99.2%, TEM, 30nm) and Co3O4 (99%, TEM, 10–30nm), were taken. The E. coli was cultured at 37˚C overnight using Luria-Bertani (LB) broth. Cultures were centrifuged at 3000g for 10min and resuspended in sterilized physiological saline. Densities of cultures of bacteria were adjusted to $0.5\times10^{9}$– $1.66\text{-}10^{9}$ cells/mL as determined by enumeration of colony forming units on LB Petri dishes.

Cytotoxicity of nanoparticles were expressed in terms of the negative logarithm of EC50, which is the effective concentration of a given oxide that reduces viability of cells of bacteria by 50%
·Heterotrophic mineralization of glucose by bacteria

was also identified as a measure of the rate of metabolism of the selected samples. After being washed three times with physiological saline, 0.1mL suspensions of E. coli were added to 2mL of distilled water solution at the nominal concentrations of 200, 400, and 600mg/L, respectively. To ensure dispersal of nanoparticles, stock solutions were prepared at a concentration of 1.2g/L after sonication at 25C for 20min. Suspensions were sonicated again for 10min just before commencement of the exposure experiments. Both control and experimental groups were then agitated for 2h at 150rpm. Rates of metabolism were measured by quantification of $^{14}CO_2$ released during metabolic respiration of uniformly radioactive label UL-$^{14}$C-D-glucose dissolved in ethanol following the 2h incubation period.

At time zero, the 50mL glass vial was sealed with a silicone stopper, on the bottom of which was hung a needle with a folded filter paper soaked with 0.05mL of 4mol/L NaOH solution for $CO_2$ trapping. Trapping occurred overnight (8–12h) after injection with 1mol/L $H_2SO_4$ at the end of 2h incubation. Filter papers were then removed and placed in 6mL scintillation vials containing 1mL of 1mol/L NaOH. Then 3mL scintillation cocktail was added to the scintillation vials and radioactivity was quantified by counting with a liquid scintillation counter. Concentrations were calculated from disintegrations per minute (DPM) and the specific activity of the mixture. [17]

**4.2 Characterisation of metal oxide nanoparticles:**

The physicochemical properties of the MeOx NPs were analysed using transmission electronmicroscopy (TEM), dynamic light scattering (DLS), and zeta potential analysis. To obtain the original particle size of the MeOx NPs and observe their particle morphology, two drops of the NP suspension were placed on a copper mesh with a carbon film using a burette. Once the sample was dry, the nanoparticles were observed using a 200kV field emission transmission electron microscope. Dynamic light scattering (DLS) was used to test the aggregation size, and zeta potential (ZP) in the cell culture medium of MeOx NPs in 20% foetal bovine complete medium was measured on a Malvern Zetasizer Nano ZS instrument. [18]

**Research on Nano-QSAR model**

**Dataset**

In this study, 21 types of MeOx NPs were investigated, which contained five types of metal oxides, including MO, $MO_2$, $MO_3$, $M_2O_3$ and $M_3O_4$. The $LC_{50}$ value was used as an indicator to characterise the acute cytotoxicity of the MeOx NPs.The acute cytotoxicity is expressed as the decadic logarithm of the concentration of nanoparticles. [19].

**Dataset splitting**

Dataset splitting is an essential part of the development of statistically significant nano-QSAR models. The toxicity dataset was divided according to the following three principles:

- ❖ Sample selection in the test set and training set should cover all types of oxides
- ❖ The split randomly keeps the highest and lowest toxic NPs in the training set
- ❖ The dataset should be divided into training and test sets with selected into the training set for descriptor selection and model development, and the remaining 5 were selected into thetest set for assessing the predictivity of the models. [20] Optimal descriptors:

We used improved SMILE based optimal descriptors to build prediction models for the cytotoxicity of MeOx NPs. Firstly, we encoded the physicochemical characteristics of the MeOx NPs and then combined them with SMILES expressions to obtain improved SMILES- based optimal descriptors, which were calculated as follows: [21]

$$DCW = \sum CW(sk) + \sum CW(ssk) + \sum CW(ck) + \sum CW(cck)$$

Where, $S_k$ and $SS_k$ - correlation weights of the attributesck and cck -correspond to the attributes of the codes

CW (ck) and CW (cck) -the correlation weights of the features, The construction of Sk (or Ck) and SSk (or CCk) can be represented as follows:

ABCDE ..

A, B, C, D, ABCDE . AB, BC, CD, DE

Also, the following normalization equation was used for assigning the codes:

$$Norm(X_k) = \min(X_k) + X_k / \min(X_k) + \max(X_k)$$

According to the given scale (Fig. 1), the number of unique values in each parameter was less than 10; therefore, the improved SMILES-based optimal

descriptor representations could be coded by assigning a number between zero and nine in a single character. In addition, alphabet characters of A, B, C, D, E, and F were expressed as molecular weight, mass percentage of metal elements, cation charge, zeta potential, individual size, and aggregation size, respectively.

To develop nano-QSAR models, the calculation was carried out with the CORAL software [22]. The nano-QSAR model for predicting the acute cytotoxicity of MeOx NPs to A549 cells can be represented by the following equation:

$$\text{Log10 (LC50)} = C0+C1\times DCW(T*N*)$$

where, C0 and C1 are the intercept and slope.

The improved SMILES-based optimal descriptors used in this study consist of traditional SMILES descriptors and six codes for physiochemical

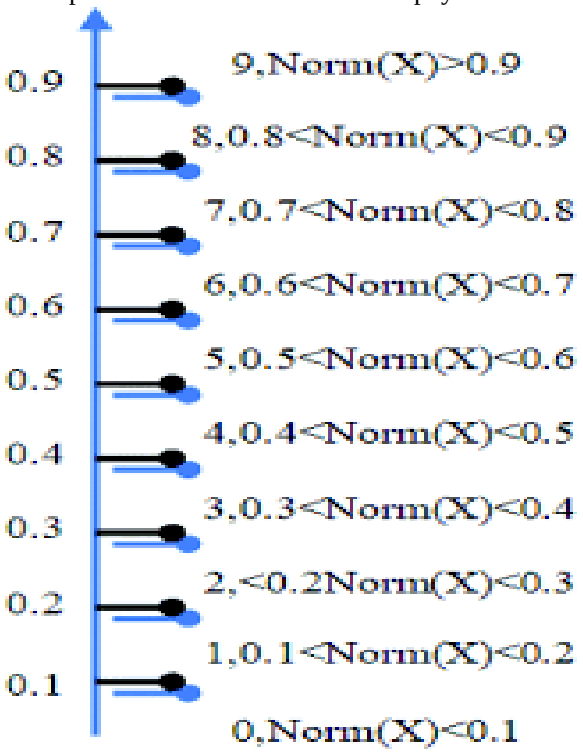


Fig. 1 Classification standards of the normalized physicochemical parameters.

Including molecular weight, mass fraction of metal atoms, zeta potential(zp), individual size (Is) aggregation size (AS), and cationic charge (CC). Data on the physicochemical features (including molecular weight, cationic charge, and mass percentage of metal elements) of various MeOx NPs can be easily obtained from their molecular formula and the periodic table.

### 5.4 Model validation:

Model validation is crucial to nano-QSAR models. The developed QSAR models were evaluated according to the standards recommended by the Organisation for Economic Cooperation and Development (OECD) [23]. Validation of the nano-QSAR models included internal verification and external verification. Internal validation was used to verify the fitting ability and robustness of the models and external validation mainly tested the predictive ability of the models for new material properties. The squared correlation coefficient ($R^2$) and standard error (SE) were employed to indicate the model fitting ability. To reduce the probability of the model's overfitting and prove the robustness of the nano-QSAR model, we applied the leave- one-out cross validation ($Q^2$ LOO) algorithm for internal validation, while the mutual validation coefficient ($Q^2$ Ext) was used for external validation. Additionally, to avoid the occurrence of accidental correlations, a Y-randomisation test was also performed to verify the reliability androbustness of the model. These reliable model criteria, was proposed by Golbraikh and Tropsha. [24]

### 5.5 Applicability domain.

According to the third principle of OECD [23], any Nano-QSAR model should have a clearly defined applicability domain (AD). Even when a model has excellent robustness and external predictivity, it still cannot reliably predict all chemicals, only those having physicochemical, structural and biological features similar to that of the training set chemicals [25]. Several methods have been proposed to define the AD of QSAR models, among which the most common is the Williams plot method [26]. In this study, the Williams plot was employed to detect the existence of influential MeOx NPs in the training set, and to verify the prediction reliability for MeOx NPs in the test set. The vertical axis of the Williams plot is the standard residual (δi). The chemicals with the absolute standard residual $|\delta| > 3$ are regarded as the Y- outliers. The horizontal axis of the Williams plot is the leverage value hi, which is defined as

$$hi = X^T i (X^T X) -1 Xi$$

where Xi is a row vector of descriptors for a particular MeOx NP

X is the n×m matrix of m model descriptors for n training set MeOx NPs

. This index is used to measure the distance between the new chemicals and chemicals in the training set. h* is the warning leverage of the application domain. The h* value can be calculated as,

$$h^*=3p/n$$

where, p is the number of variables used in the model
n is the data size of the training set.

**6. Computational Nano QSAR model:**

To explore the effects of the physicochemical structure parameters of MeOx NPs on their acute cytotoxicity, four toxicity prediction models were established, including basic Model I and Model II

Model I

Model II.

In both models, DCW is the value of the descriptor; n is the number of NPs in the training set; $R^2$ is the squared correlation coefficient; $Q^2$ LOO is the cross-validated $R^2$; SE is the standard error; F is the Fischer ratio; and p is the p-value.

Both models were then applied to predict the log10 (LC50) values of the MeOx NPs in the test set for considering particle size, Model III considering zeta potential, and Model IVconsidering both particle size and zeta potential. [27]

Here, Model I was considered a basic model that the improved the SMILES based optimal descriptor only containing three codes, MW, M%, and CC.

**Case study 1: The effect of particle size**:

Two different forms of the improved SMILES -based optimal descriptors were used to model the acute cytotoxicity to the A549 cells. The corresponding nano-QSAR models were obtainedas follows:

$$\text{Log10 (LC50)} = 0.450(\pm 0.144) + 0.136(\pm 0.006) \times \text{DCW (1,6)}$$

$$R^2 = 0.865,\ Q^2\ \text{LOO} = 0.832,\ \text{SE} = 0.210,\ F = 78,\ n = 16,\ p < 0.05$$

$$\text{Log10 (LC50)} = -4.449\ (\pm 0.117) + 0.313(\pm 0.005) \times \text{DCW (2,10)}$$

$$R^2 = 0.972,\ Q^2\ \text{LOO} = 0.962,\ \text{SE} = 0.096,\ F = 478,\ n = 16,\ p < 0.05$$

external validation.

The predicted values are shown in Table 2[28]. It can be concluded that these two models are statistically reliable. The plots of the predicted log10 (LC50) values against the experimental values for Models I and II shown in figure

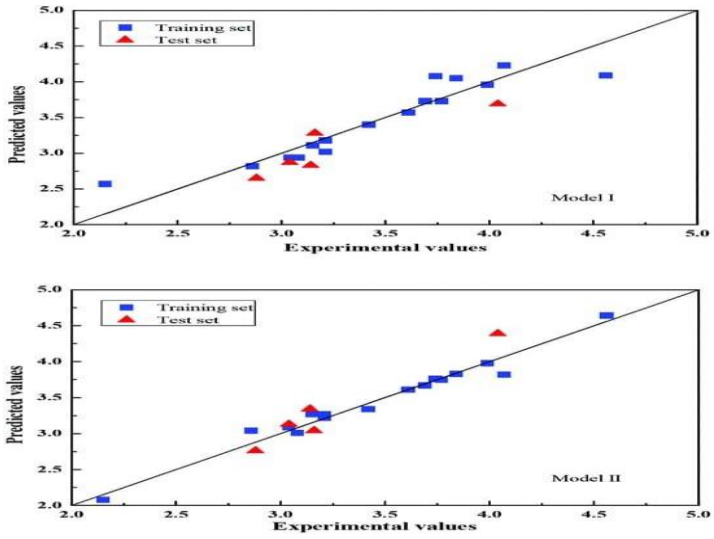


Fig2: Plot of predicted vs. experimental log10 (LC50) values for models I and II

**Case study 2: The effect of zeta potential.**
We employed the improved SMILES-based optimal descriptor with zeta potential to model the acute toxicity, and obtained the corresponding nano-QSAR model as follows:

$$\text{Log10 (LC50)} = -2.646\ (\pm\ 0.135) + 0.302(\pm\ 0.002) \times \text{DCW (2,14)}$$

$$R^2 = 0.\ 902,\ Q^2_{LOO} = 0.874,\ SE = 0.178,\ F = 178,\ n = 16,\ p < 0.05$$

The predicted log10 (LC50) values based on Model III are presented in Table 2. The plots of the predicted values against the experimental values for Model III are presented in Fig.3.

Remarkably, the performance of the parameters of Model III was superior to that of Model I.

Since both models selected the same sample set and modelling method, the difference between prediction performances mainly depended on whether the improved SMILES-based optimal descriptor considered the zeta potential.

Thus, result strongly suggests that the Zeta potential has a certain effect on the acute cytotoxicity of metal oxide nanoparticles.

| | | Model I | | Model II | | Model III | | Model IV | | |
|---|---|---|---|---|---|---|---|---|---|---|
| Metal oxide | $Log_{10}$ ($LC_{50}$) experimental value | DCW | Predicted values | DCW | Predicted value | DCW | Predicted value | DCW | Predicted value | Set |
| $Al_2O_3$ | 3.84 | 26.563 | 4.05 | 26.475 | 3.83 | 21.441 | 3.83 | 33.698 | 3.87 | Training |
| $Bi_2O_3$ | 2.86 | 17.450 | 2.82 | 23.938 | 3.04 | 20.214 | 3.29 | 27.048 | 2.86 | Training |
| $HfO_2$ | 3.77 | 24.150 | 3.73 | 26.210 | 3.75 | 21.115 | 3.73 | 33.034 | 3.75 | Training |
| $Mn_2O_3$ | 2.15 | 16.347 | 2.57 | 20.876 | 2.08 | 15.826 | 2.13 | 22.673 | 2.20 | Training |
| NiO | 3.08 | 18.326 | 2.94 | 23.838 | 3.01 | 19.019 | 3.10 | 28.445 | 3.07 | Training |
| $SiO_2$ | 3.69 | 24.147 | 3.73 | 25.965 | 3.67 | 20.811 | 3.64 | 32.356 | 3.66 | Training |
| $TiO_2$ | 3.21 | 20.123 | 3.18 | 24.528 | 3.22 | 19.621 | 3.28 | 29.014 | 3.16 | Training |
| $WO_3$ | 3.74 | 26.737 | 4.08 | 26.230 | 3.76 | 21.167 | 3.75 | 33.413 | 3.82 | Training |
| $Y_2O_3$ | 3.04 | 18.361 | 2.94 | 24.101 | 3.09 | 19.038 | 3.10 | 27.690 | 2.96 | Training |
| Zno | 3.21 | 18.933 | 3.02 | 24.674 | 3.27 | 19.406 | 3.27 | 29.484 | 3.23 | Training |
| $ZrO_2$ | 3.99 | 25.842 | 3.96 | 26.952 | 3.98 | 22.100 | 4.03 | 34.532 | 3.98 | Training |
| $Fe_2O_3$ | 3.61 | 22.975 | 3.57 | 25.778 | 3.61 | 20.395 | 3.51 | 32.064 | 3.62 | Training |
| $Gd_2O_3$ | 3.42 | 21.738 | 3.40 | 24.906 | 3.34 | 20.024 | 3.40 | 30.736 | 3.43 | Training |
| $In_2O_3$ | 4.07 | 27.908 | 4.23 | 26.439 | 3.82 | 20.214 | 3.56 | 35.041 | 4.07 | Training |
| $SnO_2$ | 4.56 | 25.744 | 4.09 | 29.059 | 4.64 | 23.958 | 4.59 | 38.086 | 4.53 | Training |
| $Yb_2O_3$ | 3.15 | 19.576 | 3.11 | 24.682 | 3.27 | 19.282 | 3.18 | 28.981 | 3.15 | Training |
| $CeO_2$ | 4.04 | 21.778 | 3.69 | 29.059 | 4.39 | 23.559 | 4.30 | 31.773 | 3.69 | Test |
| $Co_3O_4$ | 3.04 | 16.029 | 2.87 | 24.219 | 3.13 | 18.647 | 3.15 | 28.602 | 3.10 | Test |
| $La_2O_3$ | 3.14 | 15.730 | 2.83 | 25.303 | 3.34 | 20.464 | 3.37 | 28.748 | 3.32 | Test |
| $Sb_2O_3$ | 3.16 | 18.931 | 3.28 | 23.938 | 3.04 | 19.267 | 3.04 | 26.349 | 2.84 | Test |
| $Cr_2O_3$ | 2.88 | 14.479 | 2.65 | 23.058 | 2.76 | 16.638 | 2.54 | 25.188 | 2.67 | Test |

Table 2: The predicted values for the training set and test set of the different models

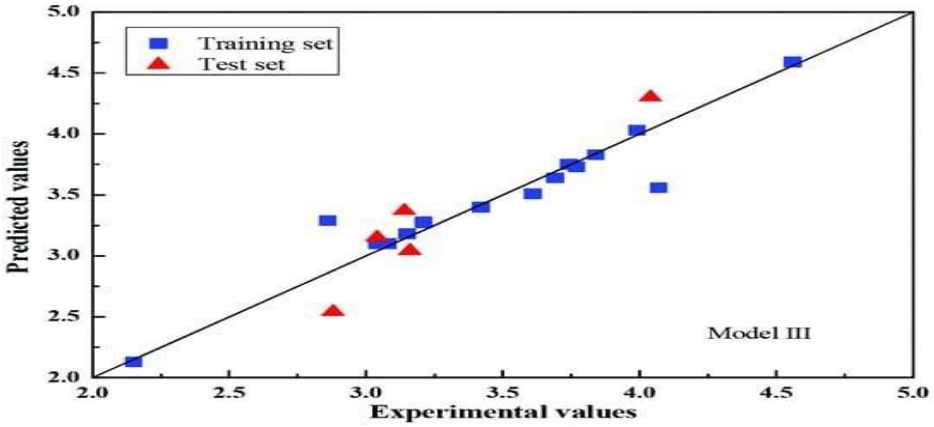


Fig.3. Plot of predicted vs experimental log10(LC50) values for model III.

**Case study 3: The effect of particle size and zeta potential:**

The improved SMILES-based optimal descriptor with particle size and zeta potential was used to model the cytotoxicity of MeOx NPs to A549 cells. The resulting nano-QSAR model was obtained as follows:

Model IV

$$\text{Log10 (LC50)} = -1.214\ (\pm\ 0.099) + 0.151(\pm\ 0.004) \times \text{DCW (1,5)}$$

$R2 = 0.996$, $Q^2$ LOO = 0.984, SE = 0.037, F = 753, n = 16, $p < 0.05$

The predicted log10 (LC50) values for Model IV are presented in Table 2. The plots of the predicted values against the experimental values for Model IV are shown in Fig.4.

Moreover, it should be noted that Model IV, which considered the particle size and zeta potential, was better than the other three models since the values of $R^2$ and $Q^2$ LOO were significantly improved.

Therefore, Model IV here shows the best goodness-of-fit and highest reliability, which indicates that particle size and zeta potential are both great influential in the acute cytotoxicity of A549 cells.

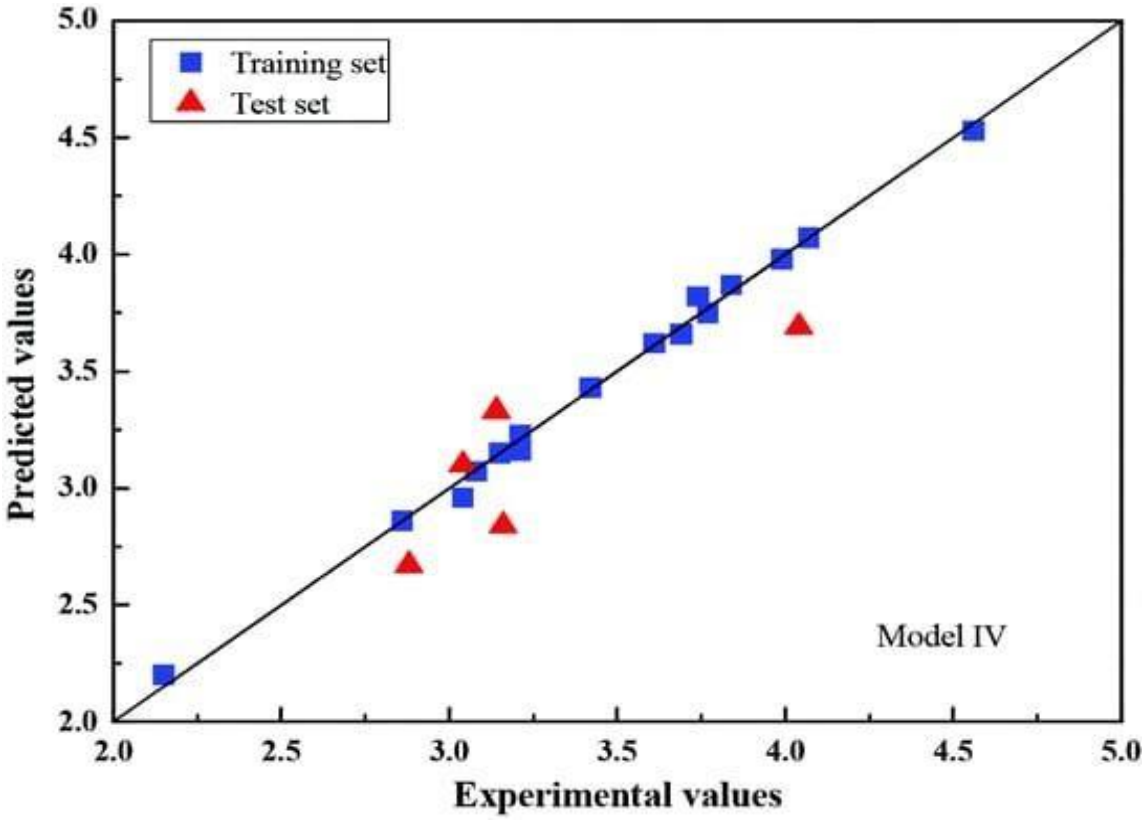


Fig.4. plot predicted vs experimental log10(LC50)values for model IV

According to the OECD QSAR verification principles, the models were fully validated because only properly validated models can provide meaningful mechanical interpretation [23]. The calculated $R^2$ values of the four models reached more than 0.8, the root means square error (RMSE) and the mean absolute error (MAE) of the predicted values were low, and the external validation coefficient $Q^2$ Ext > 0.7. Consequently, we verified that the four Nano- QSAR models all have good adaptability, robustness, and external prediction capability. To avoid the "correlation-by-chance" and confirm the statistical significance of the nano-QSAR models, Y-randomisation tests were also performed. The dependent variable y of the original dataset was randomly disordered and combined with the original independent variable to form a new dataset. Thus, a new model was established and its complex correlation coefficient was calculated. The dataset was tested 10 times for each model and the obtained $R^2$ values of the newly generated models are presented in the ESI. As expected, all the models generated produced low $R^2$ values. This indicates that only the correct dependent variables can be used to generate a real QSAR relationship and the chance correlation had little or even no effect

.

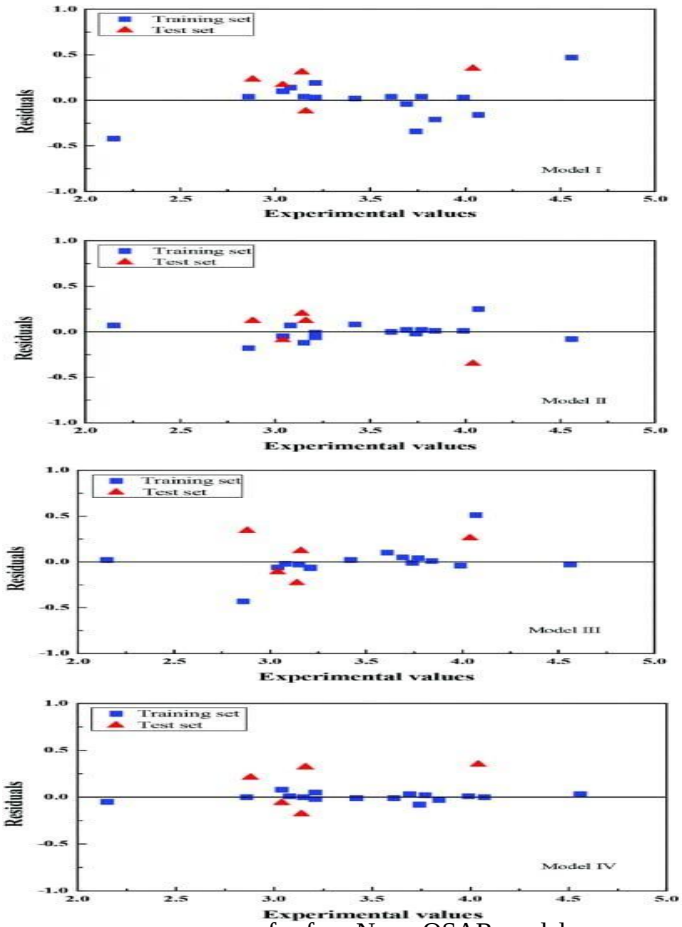


for four Nano-QSAR models

on the presented models. In addition, the residuals between the predicted and experimental log10 ($LC_{50}$) values for the four developed models are shown in Fig.5. Since most of the residuals are randomly distributed on both sides of the zero baseline without obvious regularity, it can be concluded that no systematic errors exist in the established four prediction models.

### 7. Applicability domain analysis

Since the four nano-QSAR models developed this study will probably be employed for reliably estimating the properties of newly designed MeOx NPs ,the since it may increase the confidence in predictions and allow the practical use of nano-QSAR models. The plots of the standardized residuals and leverages value (Williams plot) for the four developed models are shown in Fig. 6. The area within the warning leverage value h* = 0.375 and ±3 standard residuals were defined to illustrate the specific application range of the nano-QSAR models. As shown in Fig 6, all 21 types of MeOx NPs fall into the application domain, and the prediction values can be considered reliable.

There were no obvious outliers in both the structural similarity axis and the acute cytotoxicity predictions .

.

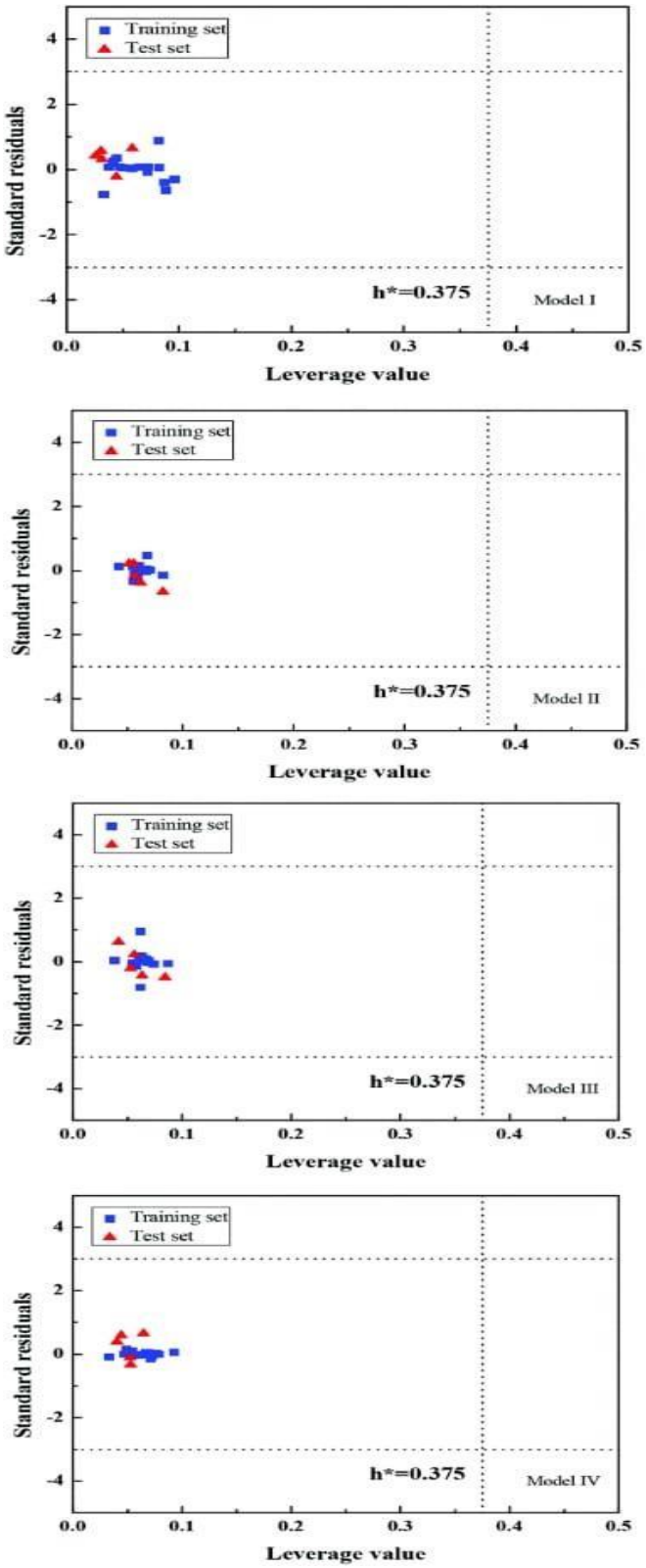

**8. Mechanism interpretation:**

In previous work, two different types of toxicity mechanisms of MeOx NPs were reported. Specifically, Mechanism I involves detachment of the metal cations from the surface of MeOx, while Mechanism II employs the redox properties of the metal oxide surface. [29][30]

In this study, the method for analysis of descriptor sensitivity combined with experiments was applied to evaluate the relative importance of each parameter on the cytotoxicity of MeOx NPs.

Six physicochemical parameters were employed to the improved SMILES-based optimal descriptors to characterise the nanostructure and develop the nano-QSAR models.

The reduced $R^2$ value was calculated when one feature is excluded from the original model. Then the differences between the original $R^2$ and the reduced ones were calculated and shown as $R^2$diff.

It is obvious that the higher value of $R^2$diff, the more the important feature. As shown in table 3, the relative importance of each parameter was ranked as: IS > AS > CC > Zp > M% > MW.

| Feature | Original $R^2$ | Reduced $R^2$ | $R^2$ diff | Rank |
|---|---|---|---|---|
| MW | 0.996 | 0.990 | 0.006 | 6 |
| M% | | 0.978 | 0.017 | 5 |
| CC | | 0.893 | 0.103 | 3 |
| IS | | 0.572 | 0.424 | 1 |
| AS | | 0.698 | 0.298 | 2 |
| ZP | | 0.972 | 0.024 | 4 |

Table.3. The difference and sorting of features in the MC-PLS model

The individual size and aggregation size were the most crucial factors for acute cytotoxicity to human cells, indicating that the size effects of MeOx NPs in the range of 11–165 nm play an important role in cytotoxicity. As the particle size decreased, the increase of the number of atoms at the MeOx NP surface suggests that more atoms will be detached from the MeOx NP surface since there are fewer chemical bonds on the surface than the interior. This interpretationsupports Mechanism I.

Another valuable factor to elucidate the cytotoxicity of MeOx NPs is cationic charge. MeOx NPs with a low cationic charge usually have strong reductive properties, and the metal cation can easily detach from the surface of the MeOx NPs, which can enhance their cytotoxicity to A549 cells. This mechanism is consistent with Mechanism I of toxicity, as discussed above. Zeta potential is another important physicochemical feature in the cytotoxicity of MeOx NPs .

Zeta potential represents the amount of charge on the particle surface, which is associated with the nanoparticle size. With a smaller particle size, the absolute value of the zeta potential increased, and the system tended to be stable. As the number of active sites on the surface increased and the cell response in the organism enhanced, MeOx NPs with opposite charges were adsorbed on the surface of cells.

The transfer of electrons disrupted the potential balance and hindered the normal exchange of substances among cells. This process is consistent with Mechanism II. The mass fraction of metal elements and molecular weight of MeOx NPs also influenced the acute cytotoxicity of A549 cells. This is mainly because the metal elements induced the A549 cells to produce ROS, which then affected the acute cytotoxicity of the MeOx NPs. Through the above analysis, we deduced that the toxicity mechanism of MeOx NPs to A549 cells is the common function of Mechanisms I and II. Moreover, according to the MADS and the ROS experiments we found that Mechanism I is more dominant than Mechanism II.

**CONCLUSION:**

A Nano-QSAR was developed to predict the cytotoxicity of metal oxide Nano particles. The present study combines experimental testing and computational modelling methodologies to explain

the toxicity of Nano-metal oxides. The model was improved by use of additional structural parameter Z/r, which increase the accuracy of prediction.

The metal oxide Nano particles (MeOxPs)were determined by biologic screening experiments to characterise the nanotoxicity of the nanoparticles. The improved SMILES-based optimal descriptors are employed to develop the corresponding nano-QSAR models for the risk assessment of MeOx NPs.

Moreover, the effects of different characteristic physicochemical properties on their acute cytotoxicity and the mechanism were discussed. All the resulting R2 and $Q^2LOO$ values of the four developed models were above 0.8, while all the external validation coefficient, $Q^2Ext$, values were above 0.7, indicating that all four developed models are reliable, stable, and with satisfactory predictive ability. Also, the applicability and reliability of the improved SMILES- based optimal descriptors for predicting the acute cytotoxicity of new MeOx NPs were verified.

In addition, the effects of structure factors on the acute cytotoxicity of MeOx NPs revealed thatthe individual size and aggregation size were the most crucial physical factors influencing the acute cytotoxicity of MeOx NPs, followed by cationic charge and zeta potential, and the effects of both metal mass fraction and molecular weight were relatively weak.

The results of the study suggest that Nano-QSARs can be a useful complementary method for hazard screening of MeONPs and their prioritization for further testing and risk assessment, and also provide information supporting the safer design of nanomaterials.

## REFERENCES:


1) Bocca, B., Caimi, S., Senofonte, O., Alimonti, A. and Petrucci, F., 2018. ICP-MS based methods to characterize nanoparticles of TiO2 and ZnO in sunscreens with focus on regulatory and safety issues. *Science of the total environment*, *630*, pp.922-930.
(2) Haas, K.H., 2021. Application of Metal Oxide Nanoparticles and their Economic Impact. Metal Oxide Nanoparticles: Formation, Functional Properties, and Interfaces, 1, pp.29-65.
(3) Hamidian, K., Saberian, M.R., Miri, A., Sharifi, F. and Sarani, M., 2021. Doped and un- doped cerium oxide nanoparticles: Biosynthesis, characterization, and cytotoxic study. Ceramics International, 47(10), pp.13895-13902.
(4) Simmons, S.O., Fan, C.Y. and Ramabhadran, R., 2009. Cellular stress response pathway system as a sentinel ensemble in toxicological screening. Toxicological sciences, 111(2),pp.202-225.
*(5)* Li, J., Wang, C., Yue, L., Chen, F., Cao, X. and Wang, Z., 2022. Nano-QSAR modeling for predicting the cytotoxicity of metallic and metal oxide nanoparticles*: A review. Ecotoxicologyand Environmental Safety, 243, p.113955.*
(6) Puzyn, T., Rasulev, B., Gajewicz, A., Hu, X., Dasari, T.P., Michalkova, A., Hwang, H.M., Toropov, A., Leszczynska, D. and Leszczynski, J., 2011. Using nano-QSAR to predict the cytotoxicity of metal oxide nanoparticles. Nature nanotechnology, 6(3), pp.175-178.
(7) De, P., Kar, S., Ambure, P. and Roy, K., 2022. Prediction reliability of QSAR models: an overview of various validation tools. Archives of Toxicology, 96(5), pp.1279-1295.
(8) Puzyn, T., Leszczynska, D. and Leszczynski, J., 2009. Toward the development of "nano-QSARs": advances and challenges. Small, 5(22), pp.2494-2509.
(9) Li, J., Wang, C., Yue, L., Chen, F., Cao, X. and Wang, Z., 2022. Nano-QSAR modeling for predicting the cytotoxicity of metallic and metal oxide nanoparticles: A review. Ecotoxicologyand Environmental Safety, 243, p.113955.
(10) Na, M., Nam, S.H., Moon, K. and Kim, J., 2023. Development of a nano-QSAR model for predicting the toxicity of nano-metal oxide mixtures to Aliivibrio fischeri. Environmental Science: Nano, 10(1), pp.325-337.
(11) Basei, G., Hristozov, D., Lamon, L., Zabeo, A., Jeliazkova, N., Tsiliki, G., Marcomini, A. and Torsello, A., 2019. Making use of available and emerging data to predict the hazards of engineered nanomaterials by means of in silico tools: A critical review. NanoImpact, 13, pp.76-99.
(12) Forest, V., Hochepied, J.F., Leclerc, L., Trouvé, A., Abdelkebir, K., Sarry, G., Augusto,V. and Pourchez, J., 2019. Towards an alternative to nano-QSAR for nanoparticle toxicity ranking in case of small datasets. Journal of Nanoparticle Research, 21, pp.1-14.
(13) Trinh, T.X., Seo, M., Yoon, T.H. and Kim, J., 2022. Developing random forest based QSAR models for predicting the mixture toxicity of TiO2 based nano-mixtures to Daphnia magna. NanoImpact, 25, p.100383.
(14) Singh, K.P. and Gupta, S., 2014. Nano-QSAR modeling for predicting biological activity of diverse nanomaterials. RSC Advances, *4*(26), pp.13215-13230.
(15) Mu Y, Wu F, Zhao Q, Ji R, Qie Y, Zhou Y, Hu Y, Pang C, Hristozov D, Giesy JP, Xing

B. Predicting toxic potencies of metal oxide nanoparticles by means of nano-QSARs. Nanotoxicology. 2016 Oct 20;10(9):1207-14.
(16) Bailer, A.J., Hughes, M.R., Denton, D.L. and Oris, J.T., 2000. An empirical comparison of effective concentration estimators for evaluating aquatic toxicity test responses. Environmental Toxicology and Chemistry: An International Journal, 19(1), pp.141-150.
(17) Aruoja, V., Pokhrel, S., Sihtmäe, M., Mortimer, M., Mädler, L. and Kahru, A., 2015. Toxicity of 12 metal-based nanoparticles to algae, bacteria and protozoa. Environmental Science: Nano, 2(6), pp.630-644.
(18) Murdock, R.C., Braydich-Stolle, L., Schrand, A.M., Schlager, J.J. and Hussain, S.M., 2008. Characterization of nanomaterial dispersion in solution prior to in vitro exposure using dynamic light scattering technique. Toxicological sciences, 101(2), pp.239-253.
(19) Singh, K.P. and Gupta, S., 2014. Nano-QSAR modeling for predicting biological activity of diverse nanomaterials. RSC Advances, 4(26), pp.13215-13230.
(20) Cao, J., Pan, Y., Jiang, Y., Qi, R., Yuan, B., Jia, Z., Jiang, J. and Wang, Q., 2020. Computer-aided nanotoxicology: risk assessment of metal oxide nanoparticles via nano- QSAR. Green Chemistry, 22(11), pp.3512-3521.
(21) Pan, Y., Li, T., Cheng, J., Telesca, D., Zink, J.I. and Jiang, J., 2016. Nano-QSAR modeling for predicting the cytotoxicity of metal oxide nanoparticles using novel descriptors. RSC advances, 6(31), pp.25766-25775.
(22) Carnesecchi, E., Toropov, A.A., Toropova, A.P., Kramer, N., Svendsen, C., Dorne, J.L. and Benfenati, E., 2020. Predicting acute contact toxicity of organic binary mixtures in honeybees (A. mellifera) through innovative QSAR models. Science of the Total Environment, 704,p.135302.
(23) Patel, M., Chilton, M.L., Sartini, A., Gibson, L., Barber, C., Covey-Crump, L., Przybylak, K.R., Cronin, M.T. and Madden, J.C., 2018. Assessment and reproducibility of quantitative structure–activity relationship models by the nonexpert. Journal of Chemical Information and Modeling, 58(3), pp.673-682.
(24) Tropsha, A., Gramatica, P. and Gombar, V.K., 2003. The importance of being earnest: validation is the absolute essential for successful application and interpretation of QSPR models. QSAR & Combinatorial Science, 22(1), pp.69-77.
(25) Gadaleta, D., Mangiatordi, G.F., Catto, M., Carotti, A. and Nicolotti, O., 2016. Applicability domain for QSAR models: where theory meets reality. International journal of quantitative structure-property relationships (IJQSPR), 1(1), pp.45-63.
(26) Zak, A.K., Majid, W.A., Abrishami, M.E. and Yousefi, R., 2011. X-ray analysis of ZnO nanoparticles by Williamson–Hall and size–strain plot methods. Solid State Sciences, 13(1), pp.251-256.
(27) Venigalla, S., Dhail, D., Ranjan, P., Jain, S. and Chakraborty, T., 2013. Computational study about cytotoxicity of metal oxide nanoparticles invoking nano-QSAR. New Front. Chem, 23, pp.123-130.
(28) Leonard, J.T. and Roy, K., 2006. On selection of training and test sets for the development of predictive QSAR models. QSAR & Combinatorial Science, 25(3), pp.235-251.
(29) Zhang, H., Ji, Z., Xia, T., Meng, H., Low-Kam, C., Liu, R., Pokhrel, S., Lin, S., Wang, X., Liao, Y.P. and Wang, M., 2012. Use of metal oxide nanoparticle band gap to develop a predictive paradigm for oxidative stress and acute pulmonary inflammation. ACS nano, 6(5), pp.4349-4368.
(30) Burello, E., 2013. Profiling the biological activity of oxide nanomaterials with mechanistic models. Computational Science & Discovery, 6(1), p.014009.